

Article ID: 1006-8775(1999) 02-0163-08

SINGULAR CROSS SPECTRUM APPLIED ON DIAGNOSTIC ANALYSIS OF AIR-SEA INTERACTION*

ZHU Yan-feng (朱艳峰), DING Yu-guo (丁裕国) and HE Jin-hai (何金海)

(*Nanjing Institute of Meteorology, Nanjing 210044 China*)

ABSTRACT: The Singular Cross Spectrum Analysis (SCSA) method was employed to investigate the coupled-periods of air-sea/mid-low circulation interaction using 1951-1993 500-hPa geopotential heights and the sea surface temperature (SST) in the Northern Hemisphere. Results show that air-sea correlation is noticeable on the 3-7 year scale which is similar to ENSO circle. In this sense, ENSO is a strong signal. Quasi-ten/quasi-four year periods are prominent in the mid-low interaction, and quasi-four year oscillation is uniform with the ENSO circle. Studies indicate that the mid-low interaction possess quasi-ten year oscillation beside being affected by ENSO.

Key words: cross singular spectrum; air-sea interaction; quasi-ten-year oscillation; ENSO

CLC number: P456.8 **Document code:** A

I. INTRODUCTION

Under the condition that physical mechanism of interaction between inside and outside of climatic system is unclear, it is important part of climatic diagnoses and prediction to discover self- and coupled-oscillation signal of various factors in different time scales. Classical cross-spectrum analysis (CSA) is a useful tool to inspect coupled-oscillation signal between two time series in frequency domain. But this method, which bases on Fourier transform theory, has its limitation. For example, its resolving power for weak coupled-signal is low; information so obtained is simple and it is also unable to quantitatively describe the feature of different coupled-oscillation signal change with time. Ding, Jiang and Shi et al. (1999) have advanced a new method (Singular-Cross Spectrum Analysis SCSA) that is applicable to analyze coupled-oscillation between two time sequences. This method can distinguish coupled-oscillation signal from two series in time domain jointly with both time and frequency domains.

As is well known, notable character of air-sea/mid-low circulation interaction is quasi-periodic. Owing to multi-scale effect of air and ocean motion, air-sea interaction is very complex. How the coupled-oscillation changes with time and the relationship between mid-low interaction and ENSO need further investigation.

In this paper, we will analyze coupled-period signal of air-sea/mid-low interaction by means of SCSA.

* **Received date:** 1998-07-08; **revised date:** 1998-12-29

Foundation item: (The paper) was supported by 《National Key Development Programme for Basic Sciences》— “Research on the Formation Mechanism and Prediction Theory of Heavy Climatic Disasters in China”, the first part of the “Research on the Foundation Mechanism and Prediction Theory of Heavy Climatic and Synoptic Disasters in China”

Biography: ZHU Yan-feng (1970 -), female, native from Xiapu City Fujian Province, doctoral student at Chinese Academy of Meteorological Sciences.

II. DATA AND METHOD

Using 1951-1993 monthly mean 500 hPa geopotential heights in the Northern Hemisphere and northern Pacific SST study coupled-signal of interaction between different regions. Zhu Yanfeng etc* analyzed coupled patterns of mid-low interaction and selected key sectors. The key oceanic sector is the tropical eastern Pacific (EP) ($10^{\circ}\text{N}-10^{\circ}\text{S}, 180^{\circ}-80^{\circ}\text{W}$), height sectors include Sector A ($10^{\circ}\text{N}-20^{\circ}\text{N}, 150^{\circ}\text{E}-150^{\circ}\text{W}$) and Region B ($40^{\circ}-50^{\circ}\text{N}, 150^{\circ}\text{E}-150^{\circ}\text{W}$). These sectors are corresponding to regions that are major distribution centers of low-frequency variability (30-60 days). Some studies indicate (Blackmon, Geisler and Pitcher et al., 1983; Li, 1995) that atmospheric motion responds primarily to changes in the tropical eastern Pacific SSTA by way of remote response and propagates to mid-high latitude through teleconnection. Therefore, analyzing coupled-period signal of interaction among aforementioned regions is beneficial to better understanding of mechanism of mid-low interaction. By taking the ensemble average of grids in the sector month by month, we establish a 516-month long set time series to represent the condition of region respectively.

Presently, observation and simulation coupled-climatic systems are heart of many preceding plans (for instance CLIVAR). Therefore, how to reveal effectively different coupled-oscillation signal is an essential problem. Cross-spectrum analysis (CSA) can reveal coupled-oscillation signal from two time series, but its shortage is that it is unable to describe different coupled-periods variation with time. Ding, Jiang, Shi et al.(1999) developed a new method which can remedy some defects of CSA. For latter reference, we introduce general algorithm of SCSA.

(1) Suppose that $\{x_t\}$, $t=1, \dots, N_x$; $\{y_t\}$, $t=1, \dots, N_y$; they are stationary time series with zero means, called left or right series respectively, being written as

$$X_{m \times N} = \begin{bmatrix} x_1 & x_2 & \cdots & x_N \\ x_2 & x_3 & \cdots & x_{N+1} \\ \cdots & \cdots & \cdots & \cdots \\ x_m & x_{m+1} & \cdots & x_{N_i} \end{bmatrix} \quad (1)$$

$$Y_{n \times N} = \begin{bmatrix} y_1 & y_2 & \cdots & y_N \\ y_2 & y_3 & \cdots & y_{N+1} \\ \cdots & \cdots & \cdots & \cdots \\ y_n & y_{n+1} & \cdots & y_{N_i} \end{bmatrix} \quad (2)$$

for the case with $m < N_i$ and $n < N_i$, cross-covariance matrix between $X(m \times N)$ and $Y(n \times N)$ is that

$$\Sigma_{xy} = \langle XY' \rangle \quad (3)$$

where $\langle \cdot \rangle$ is taking the ensemble average of $t=1, \dots, N$.

* This paper has been submitted to Acta.Meteorologica.Sinica.

(2) By singular value decomposition of the cross-covariance matrix, there have two linear combination series weighted by $L = (l_1, l_2, \dots, l_m)$ and $G = (g_1, g_2, \dots, g_n)$, corresponding to $\{x_t\}$ and $\{y_t\}$ respectively.

$$A_t = LX \quad (4)$$

$$B_t = GY \quad (5)$$

where $A_t = (a_1(t), \dots, a_p(t))'$ $t=1, \dots, N$ (6)

$$B_t = (b_1(t), \dots, b_p(t))' \quad p \leq \min(m, n) \quad (7)$$

L and G are satisfied by taking

$$LL' = I, \dots, GG' = I \quad (8)$$

Cross-covariance of A_t and B_t are maximized, which is written as

$$COV(A_t, B_t) = L' \Sigma_{xy} G = \max \quad (9)$$

Following the matrix theory, we obtain Eq.(10) from Eq.(9) that

$$L' \Sigma_{x,y} G = \begin{bmatrix} \Lambda & 0 \\ 0 & 0 \end{bmatrix} \quad (10)$$

where $\Lambda = \text{diag}(\sigma_1, \sigma_2, \dots, \sigma_p)$, $p \leq \min(m, n)$, and

$$\sigma_1 \geq \sigma_2 \geq \dots \geq \sigma_p \geq 0 \quad (11)$$

These are singular values $\sigma_i (i=1, \dots, p)$ in SVD theory, but for two-dimensional time series $\{x_t\}$ and $\{y_t\} t=1, \dots, N$, we can prove that all σ_i is kind of cross-spectrum between left and right sequence (Ding et al., 1999). Combined-series pairs $a_h(t)$ and $b_h(t) (h=1, \dots, p; t=1, \dots, N)$ associated with parameters of m, n and N are obtained by means of Eqs.(4) and (5).

(3) The percentage of covariance explained by a single pair of patterns is

$$P = \sigma_i^2 / \sum_{j=1}^r \sigma_j^2 \quad (12)$$

and the cumulative covariance fraction explained by the leading H modes is

$$P_H = \sum_{i=1}^H \sigma_i^2 / \sum_{j=1}^r \sigma_j^2 \quad (13)$$

(4) Describing time-variable feature of coupled-oscillation signal; in view of SCSA results, Eqs.(4, 5) are extended as

$$a(T_h, \tau) = \frac{1}{F_1} \int L \left(\frac{t-\tau}{T_h} \right) x(t) dt \quad (14)$$

$$b(T_h, \tau) = \frac{1}{F_2} \int G\left(\frac{t-\tau}{T_h}\right) y(t) dt \quad (15)$$

where, $L\left(\frac{t-\tau}{T_h}\right)$ and $G\left(\frac{t-\tau}{T_h}\right)$ are coupled-oscillation mode function, τ and T_h is time-migration and frequency scale parameter individually, $T_h = 2\pi/\omega_h$ corresponding h -th frequency, F_1 and F_2 are normalized factors for $x(t)$ and $y(t)$ respectively. In fact, Eqs.(14,15) indicate a kind of coupled-mode, which can be considered a typical coupled-mode function extracted from time series under certain conditions (in the SVD sense), rather than a mother-function preset in advance.

For practical purposes, we can truncate $L\left(\frac{t-\tau}{T_h}\right)$ and $G\left(\frac{t-\tau}{T_h}\right)$ into Eqs.(14, 15) to recalculate $a(T_h, \tau)$ and $b(T_h, \tau)$ by T_h , then draw up corresponding isoline pictures.

III. ANALYSIS COUPLED PERIODS INTERACTION BETWEEN AIR AND SEA

1. Analysis of coupled periods between tropical East Pacific SST and geopotential height sectors

1) CROSS SINGULAR SPECTRUM ANALYSIS

Tab. 1 lists characteristics of the first six pairs of eigenvector, which express major periodical modes and explain 86.4% of the variance. As Tab. 1 shows, the six eigenvectors correspond to three periodical modes, the first mode (44 months) which is identified by pairs 1-2 explain 27.9% and 26.9% of the variance respectively; pairs 3-4 display 68-60-month oscillation and explain 11.8% and 8.8% of the variance individually. Next is a 84-month period (pair 5-6) with a smaller variance (6.3% and 5.7%).

According to G.Plaut and R.Vautard demonstration (Plaut and Vautard, 1994), we recon-

Tab. 1: The periods estimated by SCSA with $m=160$

Pair	L=1	L=2	L=3	L=4	L=5	L=6
Periods (months)	44	44	68	60	84	84
Correlation between right and left vector	0.95	0.94	0.81	0.85	0.76	0.76
Variance %	27.9%	26.9%	11.8%	8.8%	6.3%	5.7%

struct the first six components individually. By combining pair 1 with pair 2, pair 3 with pair 4, and pair 5 with pair 6, the 44-month, 60-68-month and 84-month modes are rebuilt, respectively. Fig.1 depicts the reconstruction of each oscillation component variable with time. The amplitude of 44-month component has obvious interannual and decadal variation and exhibits wave-type disturbance (Fig.1a). The amplitude is weak before the year of 1958, then it becomes strong, but

it is relatively weak from end of the 1960's to beginning of the 1970's, and obviously increases after 1986. The variation in Sector A drops behind SST by up to six months in the 44-month period.

Before the 1980's, the amplitude of 60-68-month oscillation (Fig.1b) is weak and the variation between Sector A and SST is almost out-of-phase. After the 1980's, it obviously strengthens and height field in Sector A lags behind SST by about six months.

As Fig.1c shows, the amplitude of 84-month mode is powerful before the 1970's, afterward it becomes feeble. So far as the phase is concerned, Sector A and EP is nearly identical before the 1960's but it is out of phase after the 1980's.

In addition, we draw up the picture of coupled-mode coefficient variation with time (Figure omitted). From the figure we find that the 84-month mode is relatively strong before the 1960's, and the 44-month mode is vigorous during the 1960's to the beginning of 1980's, afterward the

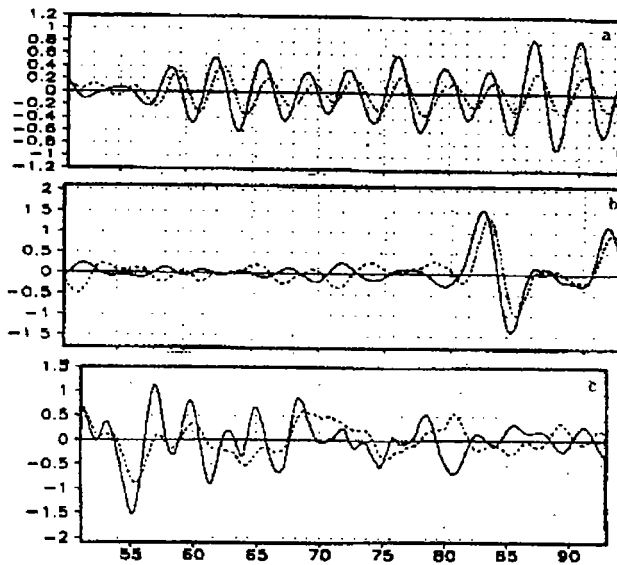


Fig. 1 Reconstruction of oscillatory components of EP-SST and geopotential heights in Sector A (dotted curves: Geopotential heights of Sector A ; solid curves: EP-SST) a:44-month component b: 60-68-month component c: 84-month component

60–68 month mode is strong. These are in good agreement with Fig.1.

2) COMPARING WITH CLASSICAL CROSS-SPECTRUM

By taking classical cross-spectrum analysis for the same data set, the SCSA results are compared and verified.

Fig.2 is the graphic description of the cross-spectrum analysis, where $M=160$ is the maximum lag, P the covariant spectrum, Q the orthogonal spectrum, and the ordinate $(P^2+Q^2)\times 100$ abscissa is the lag scale $L(0-$

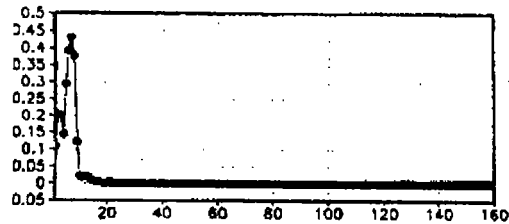


Fig.2 Cross-Spectrum graph

M) corresponding to a period from ∞ to 2 (month).

From Fig.2 we may see that the two series are closely related in the range of 32 to 106 months and the spectrum peak locates at the 45-month point. On this scale, the coagulation spectrum square is 0.92 (for in the F test, $R_c^2 = 0.53$ when $\alpha=0.05$), reaching the significance level, and Sector A lags behind EP by about 4.7 months. The coagulation spectrum square is 0.63 passing significance test, and Sector A lags behind EP by up to 4.5 months on the 64-month scale. In the 80-month range, the coagulation spectrum square is 0.57, also reaching the significance level and Sector A lags behind EP by about 2.5 months.

In the cross-spectrum graph, the six vigorous signals detected by SCSA almost concentrate in a major peak section but CSA is unable to distinguish these periods one by one. Theoretically, cross-spectrum is power spectrum in the spectrum-window sense, resolution and stability of spectrum are subject to how the spectrum windows (m) are chosen. And these usually lead to different mixed-up periods and affect the capability of CSA to distinguish signal accurately. However, SCSA is not intensively dependent on m . On the whole, major results obtain by two methods are identical. Comparing with CSA, SCSA possesses merits as follows.

(1) SCSA has stronger resolute ability than CSA and can reveal more information. For instance, we know not only the variance contribution ratio of a certain coupled-period of the interaction between the two series but also the contribution ratio of this signal of the self-oscillation.

(2) SCSA possesses distinctive characteristics in time and frequency domain. It may exhibit the component series corresponding to certain oscillation variations with time by reconstructing the oscillation components.

2. SCSA of EP-SST and B height sector

Let's study the characteristics of the first 6 pairs of eigenvectors of SCSA of EP and B (Table omitted). The first six pairs of eigenvectors express major periodical modes and their variance contribution ratio is 81.2%(Table omitted). These eigenvectors correspond to two periodical modes, where pairs 1, 2, 3, 5 and 6 express the 40-44-month mode and explain 73.8% of the variance. Pair 4 displays the 68-month mode and explains 7.4% of the variance.

We reconstruct the first six components respectively. Pairs 1, 2, 3, 5 and 6 are combined to be the 40-44-month mode and pair 4 the 68-month component. It can be seen from Fig.3a that Region B and EP variation appear in out-of-phase manner on this scale.

As Fig.3b shows, the amplitude of 60-68-mode is relatively strong before 1958 and from the 1970's to the middle of 1980's, Region B and EP variation is nearly out of phase. To sum up, prominent periods of mid-low latitude air-sea interaction are 40-84 months, which is consistent with the ENSO cycle scale. In other words, ENSO is a strong signal of mid-low latitude air-sea interaction.

3. Analyzing coupled-periods of interactions between mid and low latitudes

By taking SCSA for heights in A and B sectors, first six eigenvectors explain 61.7% of the variance and express three periodical modes. The 144-month mode, which occupies 26.2% of the variance, is identified by pair 1 and pair 5. The contribution ratio of 36-48-month mode which is identified by pairs 2, 3 and 6 is 26.0%. The fourth eigenvector corresponding to 100-month oscillation explains 9.5% of the variance.

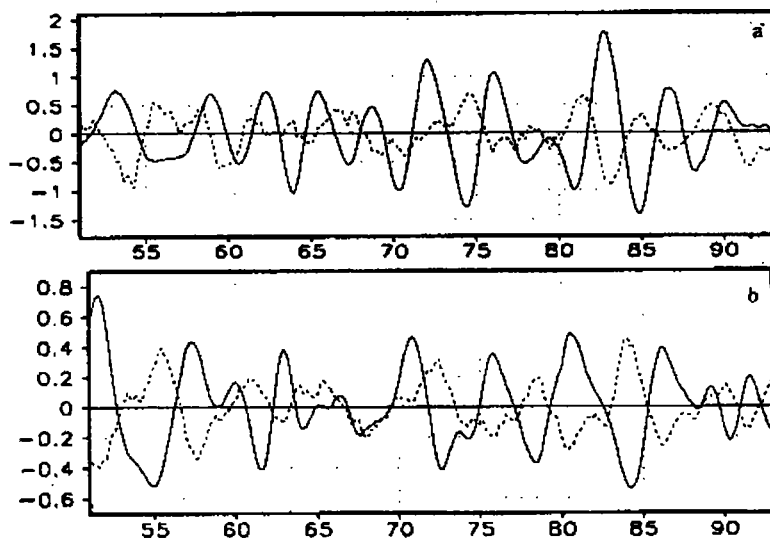


Fig.3 Reconstruction of oscillatory components of EP-SST and Geopotential heights B (dotted curves: geopotential heights B ;solid curves: EP-SST) a:44-44-month component b: 68-month component

We reconstruct first six components respectively. Combining pair 1 with pair 5, pair 2 with 3 and 6, the 144-148-month mode and 36-48-month mode are rebuilt, respectively. Pair 4 is reconstructed as the 100-month mode. Fig.4 shows the reconstruction series of each oscillation variable with time. From Fig.4a we may see that amplitude of sector B is weaker than sector A, and sectors A and B variation appear in almost out-of-phase manner, sector B lags behind A by about six months to nine months on 144-148-month scale.

The amplitude of the 36-48-month periods is weak before the 1980's (but it is relatively strong from the end of the 1950's to the beginning of the 1960's), afterward it obviously increases. Variation in sectors A and B is nearly out of phase, sector B lags behind A by up to six months (Fig.4b). The amplitude of 100-month oscillation is vigorous prior to the 1980's before it becomes feeble, and sectors A and B vary in almost an out-of-phase manner (Fig.4c).

These results indicate that the prominent periods of mid-low latitude interactions are 10-12 year and quasi-4-year, being consistent with the ENSO cycle scale. The former explains 35.7% of the variance and the latter explains 26.0% of the variance. In other words, the mid-low latitude interaction possesses quasi-ten-year oscillations beside being affected by ENSO. Studies confirm that many circle elements express quasi-ten-year oscillations (Gao and Wu, 1998). It is worth exploring the relation between air and sea variation on the quasi-ten-year scale. We find that it is different to predict decadal change of SST when we try to forecast ENSO. That indicates that decadal variability of air-sea interaction is a complex problem and needs further investigation.

IV. CONCLUDING REMARKS

a. Studies show SCSA possesses obvious merits and it may reveal more information than CSA. By taking SCSA, we know not only the contribution ratio of a certain coupled-period of the interaction between two series but also the contribution ratio of this signal of the self-oscillation. At the same time, it may exhibit the variation of a component series corresponding to

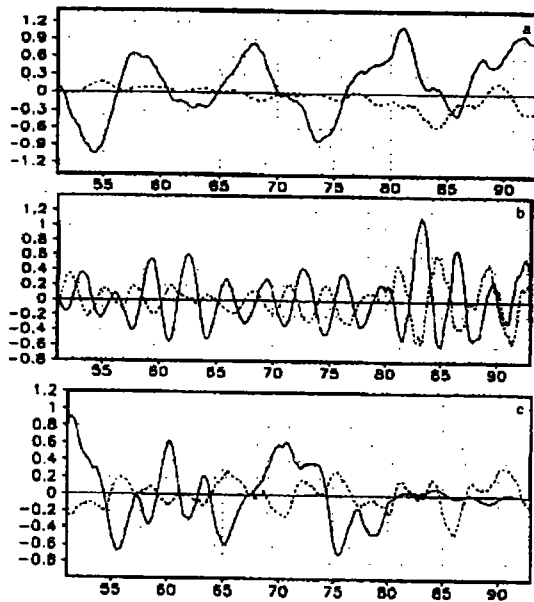


Fig.4 Reconstruction of oscillatory components of Geopotential heights A and B
 (dotted curves: region B ; solid curves: sector A) a:144-148-month component
 b: 36-48-month component c:100-month component

certain oscillations with time in terms of reconstructing the oscillation component by a joint manner with both time and frequency domains.

b. On the whole, prominent periods of mid-low latitude air-sea interaction is 40-84 month which is consistent with ENSO cycle. It shows that ENSO is a strong signal of air-sea interaction.

c. Mid-low latitude interaction exists in 10-12-year and quasi-4-year oscillation, the latter being consistent with ENSO cycle. That indicates that the mid-low latitude interaction possesses quasi-10 year oscillation beside being affected by ENSO.

REFERENCES:

- DING Yu-guo, JIANG Zhi-hong, SHI Neng, ZHU Yan-feng, 1999. Singular cross-spectrum analysis and its applicability in climatic diagnosis (in Chinese) [J]. *Sci. Atmos. Sin.*, **23**(1): 91-100.
- HOSKINS B, PEARCE R, eds., SUN Zhao-bo, TU Qi-pu, RUI Zhao-cong trans., 1987. Large-scale dynamical processes in the atmosphere [M]. Beijing: China Meteorological Press, 58-68.
- BLACKMON M L, GEISLER J E, PITCHER E J, 1983. A general circulation model study of January climate anomaly patterns associated with interannual variation of equatorial Pacific sea surface temperature [J]. *J. Atmos. Sci.*, **40**: 1414-1425.
- LI Cong-yin, 1995. Introduction to Dynamical Climatology (in Chinese) [J]. Beijing: China Meteorological Press. 104.
- PLAUT G, VAUTARD R, 1994. Spells of low-frequency oscillations and weather regimes in the Northern Hemisphere [J]. *J. Atmos. Sci.*, **51**: 210-235.
- GAO Deng-yi, WU Bing-yi, 1998. Preliminary study on decadal oscillation and its oscillation source of the sea-ice-air system in the Northern Hemisphere [J]. *Sci. Atmos. Sin.*, **22**(2): 137-144.